

# A generalization of Aztec dragons

Tri Lai\*

Institute for Mathematics and its Applications  
University of Minnesota  
Minneapolis, MN 55455  
tmlai@ima.umn.edu

Mathematics Subject Classifications: 05A15, 05C70, 05E99

## Abstract

Aztec dragons are lattice regions first introduced by James Propp, which have the number of tilings given by a power of 2. This family of regions has been investigated further by a number of authors. In this paper, we consider a generalization of the Aztec dragons to two new families of 6-sided regions. By using Kuo's graphical condensation method, we prove that the tilings of the new regions are always enumerated by powers of 2 and 3.

**Keywords:** perfect matching, tiling, Aztec dragon, graphical condensation.

## 1 Introduction

A lattice partitions the plane into *fundamental regions*. A *region* considered in this paper is a finite connected union of fundamental regions. We call the union of any two fundamental regions sharing an edge a *tile*. We would like to know how many different ways to cover a certain region by tiles so that there are no gaps or overlaps; and such coverings are called *tilings*. We use the notation  $M(R)$  for the number of tilings of a region  $R$ .

We consider a symmetric dissection of the plane into equilateral triangles, squares, and regular hexagons, with 4 polygons meeting at each vertex and with no two squares sharing an edge (see Figure 1.1). We call the resulting lattice the *dragon lattice*. James Propp introduced a family of regions called *Aztec dragons* on this lattice, which have similar structure to the classical Aztec diamonds [3]. Figures 1.1(a)–(d) show the Aztec dragons of order 1, 2, 3 and 5, respectively. James Propp realized that the number of tilings of the Aztec dragon is always a power of 2. He posed a conjecture about the tiling formula on his list of open problems in enumeration of tilings (see Problem 15 in [7]). The conjecture was first proven by Ben Wieland (in an unpublished work, as announced in [7]). However, the first published proof was given by Ciucu (see Corollary 7.2 in [1]).

**Theorem 1.1** (Aztec Dragon Theorem). *The number of tilings of the Aztec dragon of order  $n$  is  $2^{n(n+1)}$ .*

---

\*This research was supported in part by the Institute for Mathematics and its Applications with funds provided by the National Science Foundation. *Tel: (612) 624-6066*

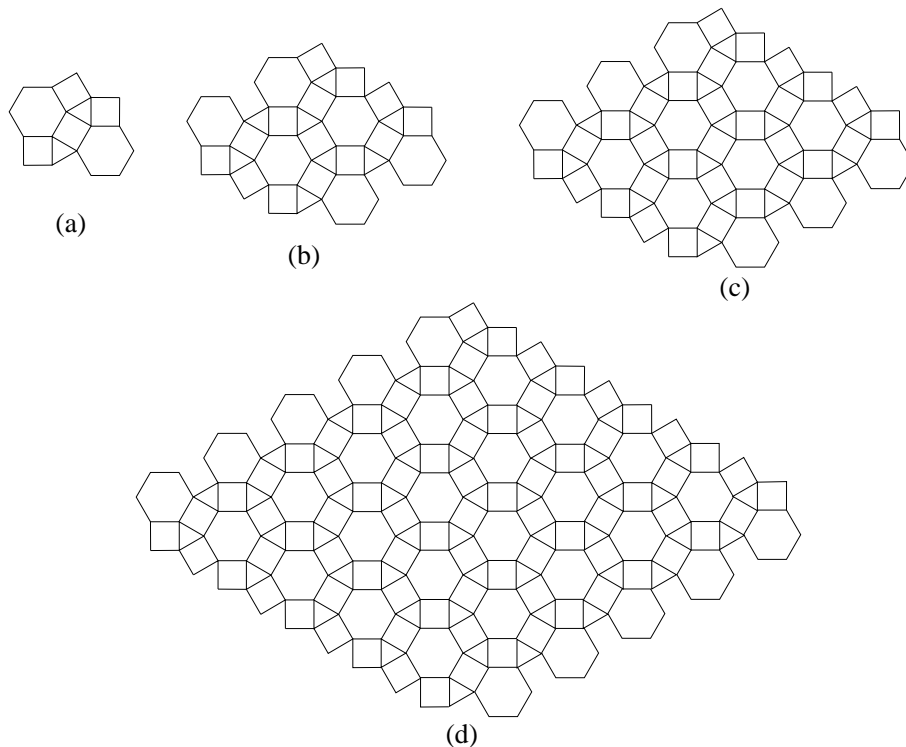


Figure 1.1: The Aztec dragons of order 1, 2, 3 and 5.

A *perfect matching* of a graph  $G$  is a collection of disjoint edges covering all vertices of  $G$ . The tilings of a region  $R$  can be identified with the perfect matchings of its *dual graph* (the graph whose vertices are fundamental regions in  $R$  and whose edges connect precisely two fundamental regions sharing an edge). In the view of this, we denote by  $M(G)$  the number of perfect matchings of a graph  $G$ . The dual graph of an Aztec dragon is called an *Aztec dragon graph*.

A further proof of the Aztec Dragon Theorem was provided in [2] by Cottrell and Young by using domino shuffling method on the Aztec dragon graphs. They also proved a related result for Aztec dragon graphs of half-integer order (see Figure 1.2). Recently, the Aztec dragon graphs have been investigated under the relations to cluster algebra (see [8] and [6]). In [6], the authors introduced a larger family of 2-parameter graphs called *Aztec castles* and proved that the numbers of perfect matchings of these graphs are always some power of 2 (see Theorem 2.1 [6]).

In this paper, we extend the family of the Aztec dragons to two new families of 6-sided regions, which we call *dragon regions* (the precise definition of a dragon region will be provided in Section 2). By using Kuo's graphical condensation method [4], we prove that the number of tilings of a dragon region is always given by powers of 2 and 3 (see Theorem 2.1). The result generalizes Aztec Dragon Theorem, as well as, the related results in [2] and [6]. Finally, in Section 5 we point out that our method can be used to obtain a related result when the tiles of the Aztec dragons carry some weights. Moreover, by the same technique, we obtain new families of regions having similar structure whose tilings are also enumerated by powers of 2 and 3.

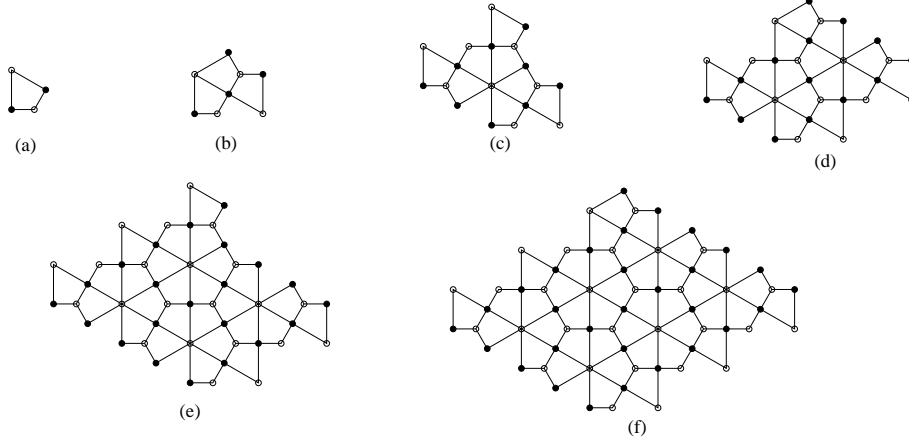


Figure 1.2: The dragon graphs of order  $n/2$  for  $1 \leq n \leq 6$ .

## 2 Dragon regions

Our goal in this section is to generalize the family of Aztec dragons.

The centers of the hexagonal fundamental regions on the dragon lattice form a triangular lattice. We consider a six-sided contour on this triangular lattice as follows.

Starting from the center  $S$  of a hexagon, we go  $a$  units<sup>1</sup> southwest,  $b$  units southeast,  $c$  units north,  $\bar{d}$  units northeast, and  $\bar{e}$  units northwest. After 5 steps, we stop at the center  $O$  of some hexagon. We adjust  $\bar{e}$  so that  $S$  and  $O$  are on the same vertical line. Finally, we close the contour by go  $\bar{f}$  units down or up depending on whether  $O$  is above or below  $S$  (see the dotted contour in Figures 2.1(a) and (b)). The above choice of  $\bar{e}$  requires

$$a + \bar{e} = b + \bar{d}. \quad (2.1)$$

The vertex  $O$  is above or below  $S$  when  $a$  is less or greater than  $c + \bar{d}$ , respectively. If  $a > c + \bar{d}$ , then the closure of the contour deduces that  $\bar{f} = a - c - \bar{d}$ ; and in the case where  $a \leq c + \bar{d}$ , the closure implies  $\bar{f} = c + \bar{d} - a$ . Thus, we always have

$$\bar{f} = |a - c - \bar{d}|. \quad (2.2)$$

Next, we consider a region with boundary running along the above contour. In particular, in the case  $a > c + \bar{d}$ , the  $b$ -,  $\bar{e}$ -, and  $\bar{f}$ -sides of the region are inside the contour (these sides have a similar structure to that of the southwest side of the Aztec dragon illustrated in Figure 1.1), and the  $a$ -,  $c$ -, and  $\bar{d}$ -sides have some hexagons protruding out halfway along the contour (this sides look like the northwest side the Aztec dragon shown in Figure 1.1). The resulting region is pictured in Figure 2.1(a). Similarly, in the case when  $a \leq c + \bar{d}$ , region stays inside the contour along its  $b$ - and  $\bar{e}$ -sides, and has some hexagons protruding out the contour along the other sides (see Figure 2.2(a)).

Color the resulting region black and white so that two fundamental regions sharing an edge have opposite color. It is easy to see that if the region admits a tiling, then the numbers of black

<sup>1</sup>The unit here is the smallest distance between the centers of two hexagonal fundamental regions in the dragon lattice, i.e the unit of the above triangular lattice.

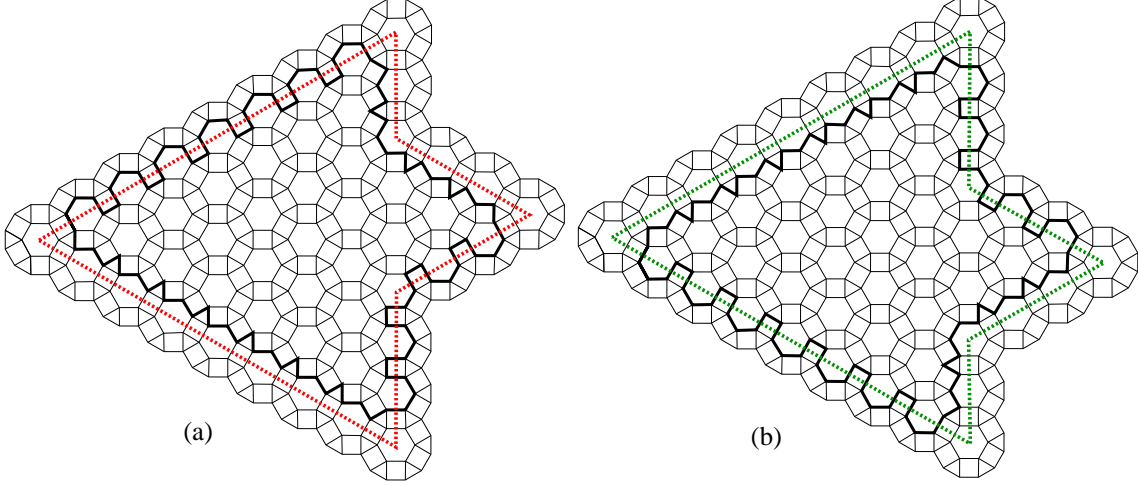


Figure 2.1: The dragon regions  $DR_{8,8,3}^{(1)}$  (a) and  $DR_{8,8,2}^{(2)}$  (b).

and white fundamental regions of its must be equal. This condition yields

$$\bar{d} = 2b - a - 2c + 1. \quad (2.3)$$

At this point, we can write  $\bar{d}, \bar{e}, \bar{f}$  all in terms of  $a, b, c$  as

$$\bar{d} = 2b - a - 2c + 1, \quad (2.4)$$

$$\bar{e} = b + \bar{d} - a = 3b - 2a - 2c + 1, \quad (2.5)$$

$$\bar{f} = |a - c - \bar{d}| = |2b - 2a - c + 1|. \quad (2.6)$$

This means that our contour and the corresponding region are determined by three parameters  $a, b, c$ . We denote by  $\mathcal{C}^{(1)}(a, b, c)$  the contour, and  $DR_{a,b,c}^{(1)}$  the region.

Next, we consider a variation  $DR_{a,b,c}^{(2)}$  of the region  $DR_{a,b,c}^{(1)}$  as follows. We define a six-sided contour similar to  $\mathcal{C}_{a,b,c}^{(1)}$  with side-lengths  $a, b, c, \tilde{d} := 2b - a - 2c - 1, \tilde{e} := 3b - 2a - 2c - 1,$  and  $\tilde{f} := |2b - 2a - c - 1|$ . Denote by  $\mathcal{C}_{a,b,c}^{(2)}$  the new contour. Similar to the constraints (2.1) and (2.2), we have  $a + \tilde{e} = b + \tilde{d}$  and  $\tilde{f} = |a - c - \tilde{d}|$ . This means that the new contour is indeed closed and has the  $\tilde{f}$ -side vertical. We now define the region  $DR_{a,b,c}^{(2)}$  with jagged boundary restricted by the contour  $\mathcal{C}^{(2)}(a, b, c)$  as in Figures 2.1(b) and 2.2(b). More precisely, if a side of  $DR_{a,b,c}^{(1)}$  is similar to the southwest side of an Aztec dragon, then the corresponding side of  $DR_{a,b,c}^{(2)}$  is similar to the *southeast* side of the Aztec dragon, and vice versa.

We call the two regions  $DR_{a,b,c}^{(1)}$  and  $DR_{a,b,c}^{(2)}$  *dragon regions*, and the dual graphs of the dragon regions *dragon graphs*. The numbers of tilings of the dragon regions are given by the theorem stated below.

**Theorem 2.1.** *Assume that  $a, b$  and  $c$  are three non-negative integers.*

(a) *If  $b \geq 2, 2b - a - 2c \geq -1$  and  $3b - 2a - 2c \geq -1$ , then*

$$M\left(DR_{a,b,c}^{(1)}\right) = 2^{(b-c+1)(2b-a-c)+(a-b)^2} 3^{\frac{(a-b+c)(a-b+c-1)}{2}}. \quad (2.7)$$

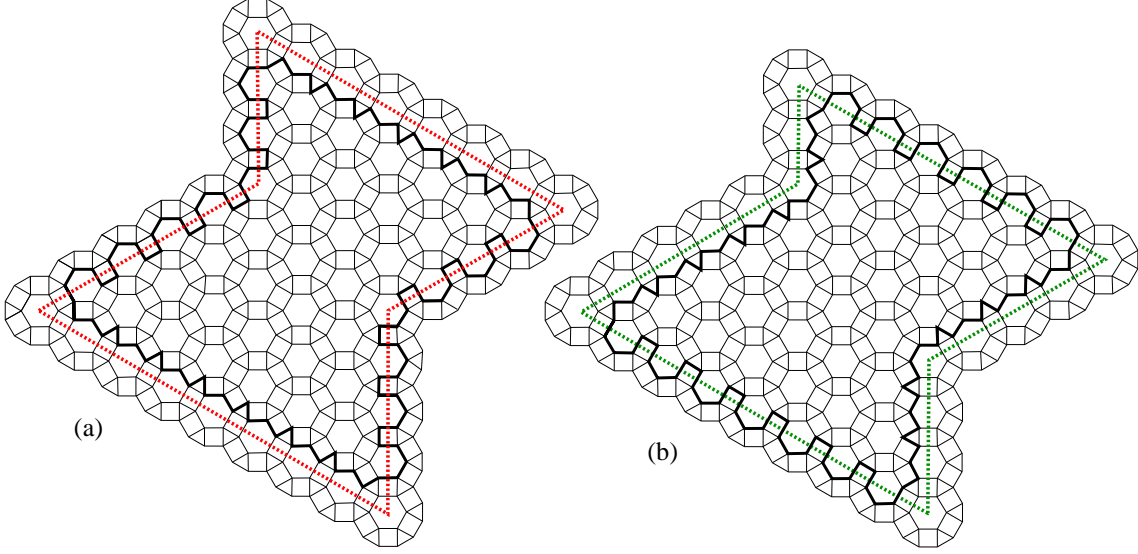


Figure 2.2: The dragon regions  $DR_{5,8,4}^{(1)}$  (a) and  $DR_{5,8,3}^{(2)}$  (b).

(b) If  $b \geq 2$ ,  $2b - a - 2c \geq 1$  and  $3b - 2a - 2c \geq 1$ , then

$$M\left(DR_{a,b,c}^{(2)}\right) = 2^{(b-c-1)(2b-a-c)+(a-b)^2} 3^{\frac{(a-b+c)(a-b+c+1)}{2}}. \quad (2.8)$$

We note that we assume the condition  $b \geq 2$  in Theorem 2.1 to guarantee that our regions are not empty.

The Aztec dragon of order  $n$  is exactly the region  $DR_{n,n,0}^{(1)}$ , thus the Aztec dragon Theorem is a consequence of Theorem 2.1. Moreover, the Aztec dragon graph of order  $n + \frac{1}{2}$  is isomorphic to the dual graph of the region  $DR_{n+1,n+2,1}^{(2)}$ , so our theorem has Cottrel and Young's theorem (Theorem 1 in [2]) as a special case.

We conclude this section by noticing that the Aztec castles in [6] corresponds to the dual graphs of the dragon regions  $DR_{a,b,c}^{(i)}$ 's, where  $a - b + c$  is  $-1$  or  $0$ .

### 3 Recurrences for the numbers of tilings of dragon regions

Consider the following system of recurrences. Here, we use the notations  $\star(a, b, c)$  and  $\diamond(a, b, c)$  for some functions from  $\mathbb{Z}^3$  to  $\mathbb{Z}$ .

$$\begin{aligned} \star(a, b, c)\star(a-3, b-3, c-2) &= \star(a-2, b-1, c)\star(a-1, b-2, c-2) \\ &+ \star(a-1, b-1, c-1)\star(a-2, b-2, c-1). \end{aligned} \quad (R1)$$

$$\star(a, b, c)\star(a-2, b-2, c) = \star(a-1, b-1, c)^2 + \star(a, b, c+1)\star(a-2, b-2, c-1). \quad (R2)$$

$$\begin{cases} \star(a, b, 0)\star(a-2, b-2, 0) = \star(a-1, b-1, 0)^2 + \star(a, b, 1)\diamond(3b-2a+1, 2b-a+1, 1); \\ \diamond(a, b, 0)\diamond(a-2, b-2, 0) = \diamond(a-1, b-1, 0)^2 + \diamond(a, b, 1)\star(3b-2a-1, 2b-a-1, 1). \end{cases} \quad (\text{R3})$$

$$\begin{aligned} \star(a, b, c)\star(a-2, b-3, c-2) &= \star(a-1, b-1, c)\star(a-1, b-2, c-2) \\ &+ \star(a-2, b-2, c-1)\star(a, b-1, c-1). \end{aligned} \quad (\text{R4})$$

$$\begin{aligned} \star(a, b, c)\star(a-2, b-3, c-2) &= \star(c, b-1, a-1)\star(a-1, b-2, c-2) \\ &+ \star(a-2, b-2, c-1)\star(a, b-1, c-1). \end{aligned} \quad (\text{R5})$$

In the next part of the section, we prove that  $M\left(DR_{a,b,c}^{(1)}\right)$  and  $M\left(DR_{a,b,c}^{(2)}\right)$  satisfy the above recurrences (with certain constraints). Our proofs are based on the following Kuo's Condensation Theorem.

**Theorem 3.1** (Kuo [4]). *Let  $G = (V_1, V_2, E)$  be a planar bipartite graph in which  $|V_1| = |V_2|$ . Assume that  $u, v, w$  and  $t$  are four vertices appearing in a cyclic order on a face of  $G$  with  $u, w \in V_1$  and  $v, t \in V_2$ . Then*

$$M(G)M(G - \{u, v, w, t\}) = M(G - \{u, v\})M(G - \{w, t\}) + M(G - \{t, u\})M(G - \{v, w\}). \quad (3.1)$$

**Lemma 3.2.** *Let  $a, b, c$  be non-negative integers so that  $b \geq 5$  and  $c \geq 2$ . Assume in addition that  $\bar{d} := 2b - a - 2c + 1 \geq 0$  and  $\bar{e} := 3b - 2a - 2c + 1 \geq 0$ . Then  $M\left(DR_{a,b,c}^{(1)}\right)$  satisfies the recurrence (R1).*

*Analogously,  $M\left(DR_{a,b,c}^{(2)}\right)$  satisfies the recurrence (R1), when  $\tilde{d} := 2b - a - 2c - 1 \geq 0$  and  $\tilde{e} := 3b - 2a - 2c - 1 \geq 0$ .*

*Proof.* To prove that  $M\left(DR_{a,b,c}^{(1)}\right)$  satisfies the recurrence (R1), we need to show that

$$\begin{aligned} M\left(DR_{a,b,c}^{(1)}\right)M\left(DR_{a-3,b-3,c-2}^{(1)}\right) &= M\left(DR_{a-2,b-1,c}^{(1)}\right)M\left(DR_{a-1,b-2,c-2}^{(1)}\right) \\ &+ M\left(DR_{a-1,b-1,c-1}^{(1)}\right)M\left(DR_{a-2,b-2,c-1}^{(1)}\right). \end{aligned} \quad (3.2)$$

We now apply the Kuo's Condensation Theorem 3.1 to the dual graph  $G$  of the regions  $DR_{a,b,c}^{(1)}$  with the four vertices  $u, v, w, t$  chosen as in Figure 3.1(a). More precisely, we chose  $u$  and  $t$  on the west corner,  $v$  on the north corner, and  $w$  on the south corner of the graph. Each of the graphs  $G - \{u, v, w, t\}$ ,  $G - \{u, v\}$ ,  $G - \{w, t\}$ ,  $G - \{t, u\}$ , and  $G - \{v, w\}$  has some edges that are forced in any perfect matchings. Fortunately, by removing these edges, we get a new dragon graph having the same number of perfect matchings as the original graph. In particular, after removing forced edges from  $G - \{u, v\}$ , we get the dual graph of  $DR_{a-2,b-1,c}^{(1)}$  (see Figure 3.1(b); the forced edges are the dark bold ones; and the dual graph of  $DR_{a-2,b-1,c}^{(1)}$  is illustrated by the one restricted by the light bold contour). Thus, we have

$$M(G - \{u, v\}) = M\left(DR_{a-2,b-1,c}^{(1)}\right). \quad (3.3)$$

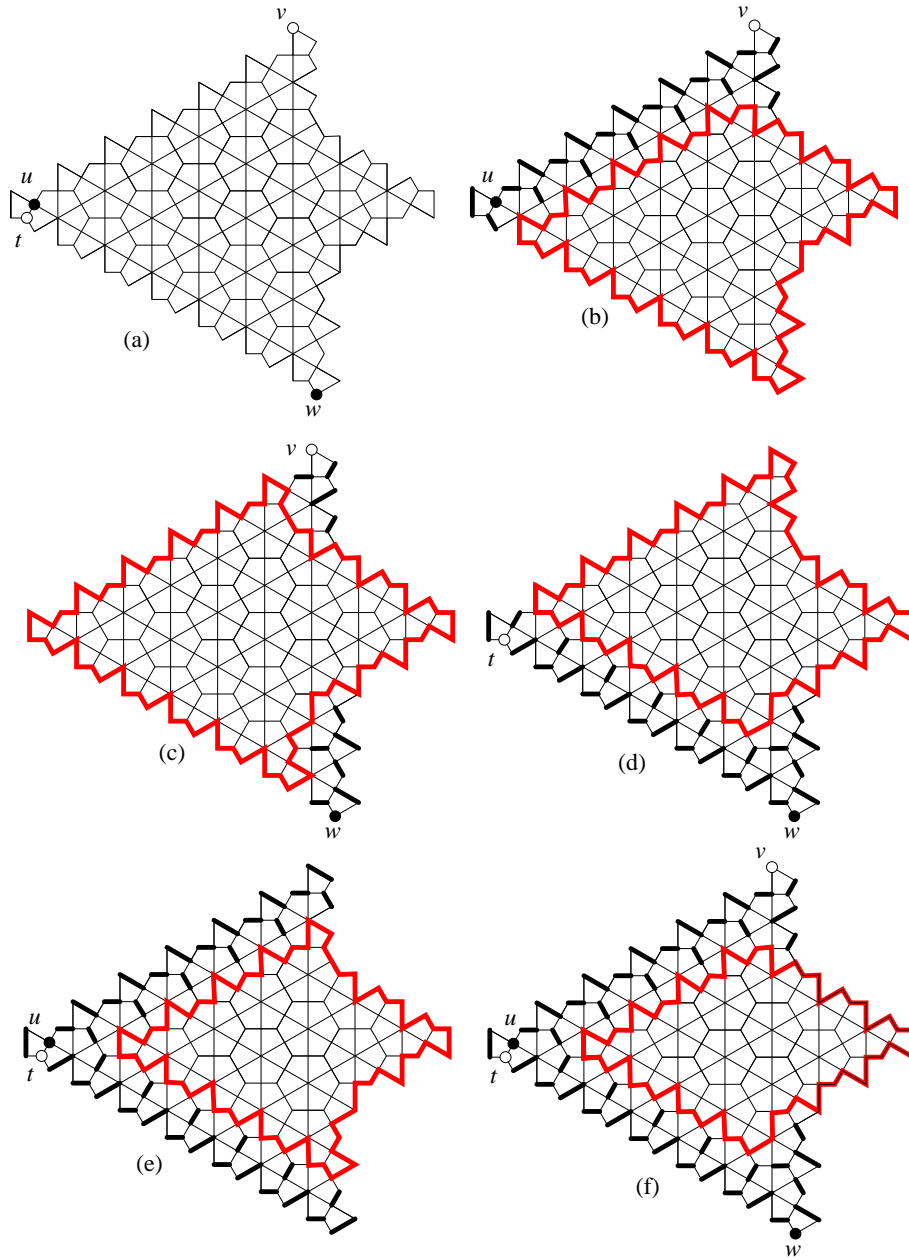


Figure 3.1: Verifying  $M(DR_{a,b,c}^{(1)})$  satisfies the recurrence (R1). The dark bold edges indicate the forced ones.

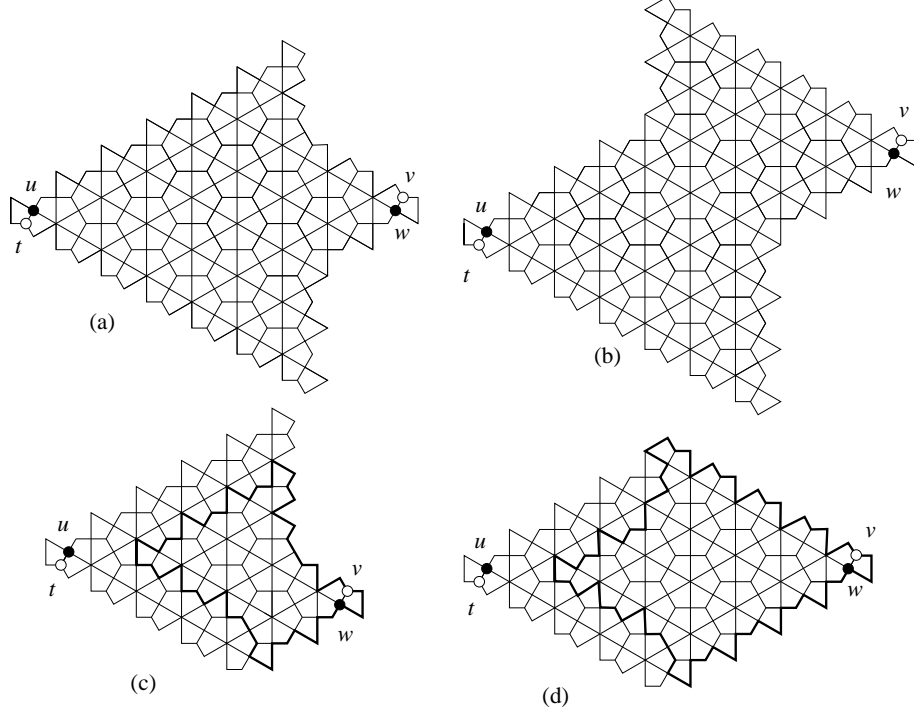


Figure 3.2: The dual graphs of (a)  $DR_{8,8,3}^{(1)}$ , (b)  $DR_{5,8,4}^{(1)}$ , (c)  $DR_{7,5,0}^{(1)}$  and (d)  $DR_{6,5,0}^{(1)}$ , together with the selection of the four vertices  $u, v, w, t$ .

Similarly, we get the following equalities:

$$M(G - \{v, w\}) = M(DR_{a-1, b-1, c-1}^{(1)}) \quad (\text{see Figure 3.1(c)}), \quad (3.4)$$

$$M(G - \{w, t\}) = M(DR_{a-1, b-2, c-2}^{(1)}) \quad (\text{see Figure 3.1(d)}), \quad (3.5)$$

$$M(G - \{t, u\}) = M(DR_{a-2, b-2, c-1}^{(1)}) \quad (\text{see Figure 3.1(e)}), \quad (3.6)$$

and

$$M(G - \{u, v, w, t\}) = M(DR_{a-3, b-3, c-2}^{(1)}) \quad (\text{see Figure 3.1(f)}). \quad (3.7)$$

Substituting, the above five equalities (3.3)–(3.7) into the equation (3.1) in Kuo's Theorem 3.1, we obtain (3.2).

The statement for the region  $DR_{a,b,c}^{(2)}$  can be obtained similarly.  $\square$

**Lemma 3.3.** *Let  $a, b, c$  be non-negative integers so that  $a \geq 2$  and  $b \geq 4$ .*

(a) *Assume that  $c \geq 1$ . Then  $M(DR_{a,b,c}^{(1)})$  satisfies the recurrence (R2), when  $\bar{d} := 2b - a - 2c + 1 \geq 2$  and  $\bar{e} := 3b - 2a - 2c + 1 \geq 2$ ; and  $M(DR_{a,b,c}^{(2)})$  satisfies the recurrence (R2), when  $\tilde{d} := 2b - a - 2c - 1 \geq 2$  and  $\tilde{e} := 3b - 2a - 2c - 1 \geq 2$ .*

(b) *Assume that  $c = 0$ . Then the pair of numbers of tilings  $(M(DR_{a,b,c}^{(1)}), M(DR_{a,b,c}^{(2)}))$  satisfies the first equality in the recurrence (R3), when  $\bar{d} := 2b - a - 2c + 1 \geq 2$  and  $\bar{e} := 3b - 2a - 2c + 1 \geq 2$ .*



2, *i.e.*

$$\begin{aligned} M\left(DR_{a,b,0}^{(1)}\right) M\left(DR_{a-2,b-2,0}^{(1)}\right) &= M\left(DR_{a-1,b-1,0}^{(1)}\right)^2 \\ &+ M\left(DR_{a,b,1}^{(1)}\right) M\left(DR_{3b-2a+1,2b-a+1,1}^{(2)}\right); \end{aligned} \quad (3.8)$$

and it satisfies the second equality of (R3), when  $\tilde{d} := 2b - a - 2c - 1 \geq 2$  and  $\tilde{e} := 3b - 2a - 2c - 1 \geq 2$ , *i.e.*

$$\begin{aligned} M\left(DR_{a,b,0}^{(2)}\right) M\left(DR_{a-2,b-2,0}^{(2)}\right) &= M\left(DR_{a-1,b-1,0}^{(2)}\right)^2 \\ &+ M\left(DR_{a,b,1}^{(2)}\right) M\left(DR_{3b-2a-1,2b-a-1,1}^{(1)}\right). \end{aligned} \quad (3.9)$$

*Proof.* (a) Similar to Lemma 3.2, we apply Kuo's Theorem 3.1 to the dual graph  $G$  of  $DR_{a,b,c}^{(1)}$  with the four vertices  $u, v, w, t$  chosen as in Figures 3.2(a) and (b), for the cases  $a > c + d$  and  $a \leq c + d$ , respectively. By considering forced edges, we get in both cases that

$$M(G - \{u, v\}) = M\left(DR_{a-1,b-1,c}^{(1)}\right), \quad (3.10)$$

$$M(G - \{v, w\}) = M\left(DR_{a,b,c+1}^{(1)}\right), \quad (3.11)$$

$$M(G - \{w, t\}) = M\left(DR_{a-1,b-1,c}^{(1)}\right), \quad (3.12)$$

$$M(G - \{t, u\}) = M\left(DR_{a-2,b-2,c-1}^{(1)}\right), \quad (3.13)$$

and

$$M(G - \{u, v, w, t\}) = M\left(DR_{a-2,b-2,c}^{(1)}\right). \quad (3.14)$$

Again, substituting (3.10)–(3.14) into the equation (3.1) in Kuo's Theorem 3.1, we deduce

$$M\left(DR_{a,b,c}^{(1)}\right) M\left(DR_{a-2,b-2,c}^{(1)}\right) = M\left(DR_{a-1,b-1,c}^{(1)}\right)^2 + M\left(DR_{a,b,c+1}^{(1)}\right) M\left(DR_{a-2,b-2,c-1}^{(1)}\right), \quad (3.15)$$

which implies that  $M\left(DR_{a,b,c}^{(1)}\right)$  satisfies the recurrence (R2). Similarly, we can prove that the number tilings of  $DR_{a,b,c}^{(2)}$  satisfies (R2).

(b) We present here the proof of (3.8), and (3.9) can be treated in the same way.

Similar to part (a), we apply the Kuo's Theorem to the dual graph  $G$  of  $DR_{a,b,0}^{(1)}$ , as in Figures 3.2(c) and (d) for the cases  $a > c + d$  and  $a \leq c + d$ , respectively. We still get the equalities (3.10), (3.11), (3.12), and (3.14) as in part (a). However, after removing forced edges from the graph  $G - \{t, u\}$ , we do *not* get the dual graph of the region  $DR_{a-2,b-2,c-1}^{(1)}$  any more (this region does *not* even exist when  $c = 0$ ). By reflecting the resulting graph about a vertical line, we get the dual graph of  $DR_{e,d,1}^{(2)}$  (see the graphs restricted by the bold contours in Figures 3.2(c) and (d)). Thus, (3.8) follows from Kuo's Theorem 3.1.  $\square$

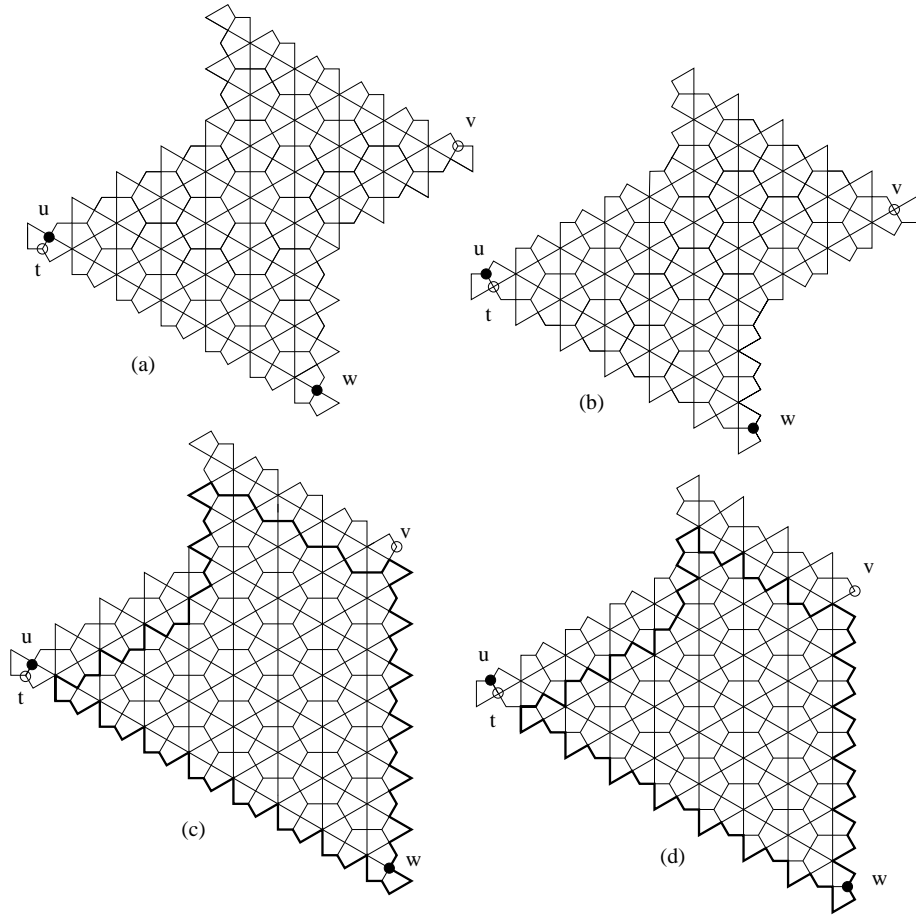


Figure 3.3: The dual graphs of (a)  $DR_{5,8,4}^{(1)}$ , (b)  $DR_{5,8,3}^{(2)}$ , (c)  $DR_{5,10,8}^{(1)}$  and (d)  $DR_{5,10,7}^{(2)}$ , together with the selection of the four vertices  $u, v, w, t$ .

**Lemma 3.4.** Assume that  $a, b, c$  are non-negative integers so that  $a \geq 2$ ,  $b \geq 5$  and  $c \geq 2$ . Denote by  $\bar{d} := 2b - a - 2c + 1$ ,  $\bar{e} := 3b - 2a - 2c + 1$ ,  $\tilde{d} := 2b - a - 2c - 1$ , and  $\tilde{e} := 3b - 2a - 2c - 1$  as usual.

(a) Assume in addition that  $\bar{d} \geq 1$ ,  $\bar{e} \geq 0$ , and  $a \leq c + \bar{d}$ , then  $M\left(DR_{a,b,c}^{(1)}\right)$  satisfies the recurrence (R4). The number of tilings  $M\left(DR_{a,b,c}^{(2)}\right)$  also satisfies the recurrence (R4), when  $\tilde{d} \geq 1$ ,  $\tilde{e} \geq 0$ , and  $a \leq c + \tilde{d}$ .

(b) If  $\bar{d} = 0$ ,  $\bar{e} \geq 0$ , and  $a \leq c + \bar{d}$ , then  $M\left(DR_{a,b,c}^{(1)}\right)$  satisfies the recurrence (R5). Analogously,  $M\left(DR_{a,b,c}^{(2)}\right)$  also satisfies the recurrence (R5), when  $\tilde{d} = 0$ ,  $\tilde{e} \geq 0$ , and  $a \leq c + \tilde{d}$ .

*Proof.* (a) To prove that  $M\left(DR_{a,b,c}^{(i)}\right)$  satisfies (R4) (with the corresponding constraints), for  $i = 1, 2$ , we apply Kuo's Theorem 3.1 to the dual graph  $G$  of the region with the four vertices  $u, v, w, t$  chosen as in Figures 3.3(a) and (b) (for the case  $i = 1$  and 2, respectively). We need to show that

$$\begin{aligned} M\left(DR_{a,b,c}^{(i)}\right) M\left(DR_{a-2,b-3,c-2}^{(i)}\right) &= M\left(DR_{a-1,b-1,c}^{(i)}\right) M\left(DR_{a-1,b-2,c-2}^{(i)}\right) \\ &\quad + M\left(DR_{a-2,b-2,c-1}^{(i)}\right) M\left(DR_{a,b-1,c-1}^{(i)}\right). \end{aligned} \quad (3.16)$$

Similar to the proofs of Lemmas 3.2 and 3.3, by removing edges forced by the removal of the vertices  $u, v, w, t$ , we get new dragon graphs. To precise, we have

$$M(G - \{u, v\}) = M\left(DR_{a-1,b-1,c}^{(i)}\right), \quad (3.17)$$

$$M(G - \{v, w\}) = M\left(DR_{a,b-1,c-1}^{(i)}\right), \quad (3.18)$$

$$M(G - \{w, t\}) = M\left(DR_{a-1,b-2,c-2}^{(i)}\right), \quad (3.19)$$

$$M(G - \{t, u\}) = M\left(DR_{a-2,b-2,c-1}^{(i)}\right), \quad (3.20)$$

and

$$M(G - \{u, v, w, t\}) = M\left(DR_{a-2,b-3,c-2}^{(i)}\right). \quad (3.21)$$

Then the equality (3.16) follows also from Kuo's Theorem 3.1.

(b) First, we note that if  $\bar{d} := 2b - a - 2c + 1 = 0$ , then  $2(b-1) - (a-1) - 2c + 1 = -1$ . This means that the region  $DR_{a-1,b-1,c}^{(1)}$  does *not* exist when  $\bar{d} = 0$ . Similarly, the region  $DR_{a-1,b-1,c}^{(2)}$  does not exist when  $\tilde{d} = 0$ . In particular, the equality (3.17) in part (a) is *not* true anymore when  $\bar{d} = 0$  or  $\tilde{d} = 0$ .

This part can be treated similarly to part (a). We still apply the Kuo's Theorem to the dual graph  $G$  of  $DR_{a,b,c}^{(i)}$  with the four vertices  $u, v, w, t$  selected as in Figures 3.3(c) and (d). We also obtain the five equalities (3.18)–(3.21) as in part (a). However, after removing forced edges from the graph  $G - \{u, v\}$ , we reflect the resulting graph about vertical line and get the dual graph of  $DR_{c,b-1,a-1}^{(i)}$  (see the graphs restricted by the bold contours in Figures 3.3(c) and (d)). Thus, we have

$$M(G - \{u, v\}) = M\left(DR_{c,b-1,a-1}^{(i)}\right) \quad (3.22)$$

instead of (3.17) in part (a). By substituting (3.18)–(3.22) into (3.1), we get the statement in part (b).  $\square$

Denote respectively by  $\Phi(a, b, c)$  and  $\Psi(a, b, c)$  the expressions on the right-hand sides of the equalities (3.2) and (3.3), i.e.

$$\Phi(a, b, c) := 2^{(b-c+1)(2b-a-c)+(a-b)^2} 3^{\frac{(a-b+c)(a-b+c-1)}{2}} \quad (3.23)$$

and

$$\Psi(a, b, c) := 2^{(b-c-1)(2b-a-c)+(a-b)^2} 3^{\frac{(a-b+c)(a-b+c+1)}{2}}. \quad (3.24)$$

It is straightforward to verify the following result.

**Lemma 3.5.** *For any integers  $a, b, c$  the functions  $\Phi(a, b, c)$  and  $\Psi(a, b, c)$  satisfy all the recurrences (R1)–(R5). In particular,  $\Phi$  and  $\Psi$  act respectively the roles of  $\star$  and  $\diamond$  in the recurrence (R3).*

## 4 Proof of Theorem 2.1

We show that

$$M\left(DR_{a,b,c}^{(1)}\right) = \Phi(a, b, c), \quad (4.1)$$

for  $b \geq 2$ ,  $\bar{d} \geq 0$ ,  $\bar{e} \geq 0$ , and that

$$M\left(DR_{a,b,c}^{(2)}\right) = \Psi(a, b, c), \quad (4.2)$$

for  $b \geq 2$ ,  $\tilde{d} \geq 0$ ,  $\tilde{e} \geq 0$ , by induction on the the perimeters of the contours of the regions. In this proof, we always denote by  $\bar{d} := 2b - c - 2a + 1$ ,  $\bar{e} := 3b - 2a - 2c + 1$ ,  $\bar{f} := |2b - 2a - c + 1|$ ,  $\tilde{d} := 2b - c - 2a - 1$ ,  $\tilde{e} := 3b - 2a - 2c - 1$ , and  $\tilde{f} := |2b - 2a - c - 1|$  as usual.

Denote by  $\mathcal{P}^{(i)}(a, b, c)$  the perimeter of the contour  $\mathcal{C}^{(i)}(a, b, c)$ , for  $i = 1, 2$ . One readily sees that  $\mathcal{P}^{(1)}(a, b, c) = a + b + c + \bar{d} + \bar{e} + \bar{f} = 4b - 2c + 1$  if  $a > c + \bar{d}$ , and  $8b - 4a - 4c + 3$  otherwise. Similarly,  $\mathcal{P}^{(2)}(a, b, c)$  equals  $4b - 2c - 1$  if  $a > c + \tilde{d}$ , and  $8b - 4a - 4c - 3$  otherwise. In particular, the two parameters are both odd.

The base cases are all  $DR^{(1)}$ -regions having the triple  $(a, b, c)$  satisfying at least one of the following conditions:

- (i)  $\mathcal{P}^{(1)}(a, b, c) \leq 15$
- (ii)  $b \leq 4$
- (iii)  $c + \bar{d} \leq 2$ ;

and all  $DR^{(2)}$ -regions having the triple  $(a, b, c)$  satisfying at least one of the following conditions:

- (iv)  $\mathcal{P}^{(2)}(a, b, c) \leq 15$
- (v)  $b \leq 3$
- (vi)  $c + \tilde{d} \leq 2$ ,

It is easy to see that each of the conditions (i), (ii) and (iii) deduce we have some bounces some small upper bound for all  $a, b, c$ . Indeed, if (i) holds, we get from the triangle inequality that  $2a, 2b, 2c \leq \mathcal{P}^{(1)}(a, b, c) \leq 15$ . Thus, we get  $a, b, c \leq 7$ . Similarly, if  $b \leq 4$ , then  $\bar{d} = 2b - a - 2c + 1 \geq 0$ , this implies  $c \leq 4$ . By the same reason,  $a \leq 2b + 1 \leq 9$ . Finally, if  $c + \bar{d} \leq 2$ , then  $2b \leq a + 2c + 1 \leq a + 5 \leq (b + \bar{d}) + 5 \leq b + 7$ . Thus  $b \leq 7$ , so  $a \leq b + \bar{d} \leq 9$ .

Taking into account also the inequalities  $b \geq 2$ ,  $\bar{d} = 2b - a - 2c + 1 \geq 0$  and  $\bar{e} = 2b - 2a - 2c + 1 \geq 0$ , we get that there are 53  $DR^{(1)}$ -regions in the base cases. Similarly, there are 28  $DR^{(2)}$ -regions having the triple  $(a, b, c)$  satisfies at least one of the conditions (iv), (v) and (vi). For each of the dragon regions in the base cases, (4.1) and (4.2) can be readily checked by for example a computer package `vaxmacs`<sup>2</sup> written by David Wilson. The number of tilings of each of these dragon regions is returned in a second.

For the induction step, we assume that  $k$  is an odd integer greater than 15 and that (4.1) and (4.2) hold for any regions with perimeter less than  $k$  ( $k \geq 17$ ). By the bases cases, we only need to show that (4.1) holds for any triples  $(a, b, c)$  in the domain

$$\bar{\mathcal{D}} = \{\mathcal{P}^{(1)}(a, b, c) = k, b \geq 7, \bar{d} \geq 0, \bar{e} \geq 0, c + \bar{d} \geq 3\},$$

and that (4.2) holds for any triples  $(a, b, c)$  in the domain

$$\tilde{\mathcal{D}} = \{\mathcal{P}^{(2)}(a, b, c) = k, b \geq 7, \tilde{d} \geq 0, \tilde{e} \geq 0, c + \tilde{d} \geq 3\}.$$

Next, we partition each of  $\bar{\mathcal{D}}$  and  $\tilde{\mathcal{D}}$  into four subdomains as follows.

$$\begin{aligned} \bar{\mathcal{D}}_1 &= \bar{\mathcal{D}} \cap \{2 \leq a \leq c + \bar{d}\}; & \tilde{\mathcal{D}}_1 &= \tilde{\mathcal{D}} \cap \{2 \leq a \leq c + \tilde{d}\}; \\ \bar{\mathcal{D}}_2 &= \bar{\mathcal{D}} \cap \{a \leq 1\}; & \tilde{\mathcal{D}}_2 &= \tilde{\mathcal{D}} \cap \{a \leq 1\}; \\ \bar{\mathcal{D}}_3 &= \bar{\mathcal{D}} \cap \{a > c + \bar{d}, \bar{e} \geq \bar{d}\}; & \tilde{\mathcal{D}}_3 &= \tilde{\mathcal{D}} \cap \{a > c + \tilde{d}, \tilde{e} \geq \tilde{d}\}; \\ \bar{\mathcal{D}}_4 &= \bar{\mathcal{D}} \cap \{a > c + \bar{d}, \bar{e} < \bar{d}\}; & \tilde{\mathcal{D}}_4 &= \tilde{\mathcal{D}} \cap \{a > c + \tilde{d}, \tilde{e} < \tilde{d}\}. \end{aligned}$$

We will show that the  $M\left(DR_{a,b,c}^{(1)}\right)$  and  $\Phi(a, b, c)$ , and  $M\left(DR_{a,b,c}^{(2)}\right)$  and  $\Psi(a, b, c)$  agree in each of the above subdomains.

There are four cases to distinguish.

*Case 1:*  $(a, b, c) \in \bar{\mathcal{D}}_1 \cup \tilde{\mathcal{D}}_1$ .

First, we assume that  $(a, b, c) \in \bar{\mathcal{D}}_1$ .

We notice that the condition  $b \geq 5$  guarantees that  $\bar{e} \geq 2$ . Indeed, since we are assuming that  $a \leq c + \bar{d}$ , we have  $a \leq 2b - a - c + 1$ . By  $\bar{d} \geq 0$ , we get  $2b - a - 2c + 1 \geq 0$ . Adding the above two inequalities, we get  $3a + 3c \leq 4b + 2$ . Then,  $\bar{e} = 3b - 2a - 2c + 1 = 3b - \frac{2}{3}(3a + 3c) + 1 \geq \frac{b}{3} - \frac{1}{3} \geq \frac{4}{3}$ . Since  $\bar{e}$  is an integer,  $\bar{e} \geq 2$ .

Moreover, since we are assuming that  $c + d \geq 3$ , then at least one of  $c$  and  $\bar{d}$  greater than 2. We first assume that  $\bar{d} \geq 2$ .

*Case 1.a.*  $\bar{d} \geq 2$ .

If  $c \geq 1$ , then, by Lemmas 3.2 and 3.5,  $M(DR_{a,b,c}^{(1)})$  and  $\Phi(a, b, c)$  both satisfy the recurrence (R2). One notices that all regions other than  $DR_{a,b,c}^{(1)}$  in the equality (3.2) have perimeters strictly less than  $k$ . Thus, by induction hypothesis, we get

$$M(DR_{a-3,b-3,c-2}^{(1)}) = \Phi(a - 3, b - 3, c - 2),$$

---

<sup>2</sup>This software is available at <http://dwilson.com/vaxmacs>.

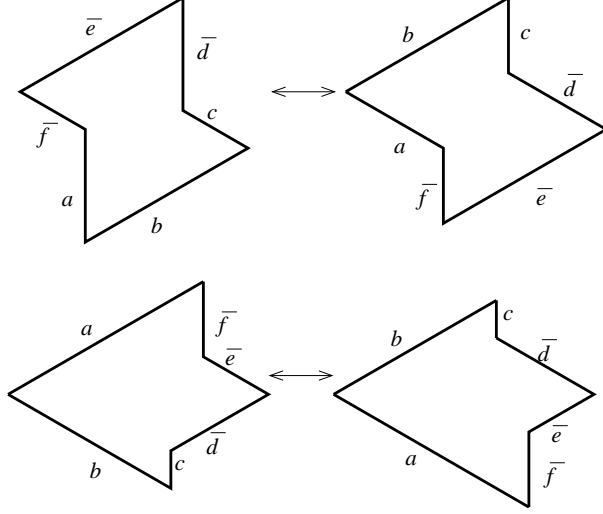


Figure 4.1: Obtaining a new hexagonal dungeon by flipping the old one.

$$M(DR_{a-2,b-1,c}^{(1)}) = \Phi(a-2, b-1, c),$$

$$M(DR_{a-1,b-2,c-2}^{(1)}) = \Phi(a-1, b-2, c-2),$$

$$M(DR_{a-1,b-1,c-1}^{(1)}) = \Phi(a-1, b-1, c-1),$$

and

$$M(DR_{a-2,b-2,c-1}^{(1)}) = \Phi(a-2, b-2, c-1).$$

By the recurrence (R2) and the above five equalities, we obtain  $M(DR_{a,b,c}^{(1)}) = \Phi(a, b, c)$ .

Similarly, if  $c = 0$ , by Lemmas 3.3(b) and 3.5, the ordered pairs  $(M(DR_{a,b,c}^{(1)}), M(DR_{a,b,c}^{(2)}))$  and  $(\Phi(a, b, c), \Psi(a, b, c))$  both satisfy the first equality in the recurrence (R3). Again, by induction hypothesis, we get (4.1).

*Case 1.b.  $c \geq 2$ .*

If  $\bar{d} \geq 1$ , then by Lemmas 3.4 and 3.5,  $M(DR_{a,b,c}^{(1)})$  and  $\Phi(a, b, c)$  both satisfy the recurrence (R4); if  $\bar{d} = 0$ , the later two functions satisfy the same recurrence (R5). Then, by induction hypothesis one more time, we get (4.1). This means that we have (4.1) for any  $(a, b, c) \in \bar{\mathcal{D}}_1$ .

In the same way, if  $(a, b, c) \in \tilde{\mathcal{D}}_1$ , we always get (4.2).

*Case 2:  $(a, b, c) \in \bar{\mathcal{D}}_2 \cup \tilde{\mathcal{D}}_2$ .*

We consider first the case when  $(a, b, c) \in \bar{\mathcal{D}}_2$ . By flipping the region  $DR_{a,b,c}^{(1)}$  about the  $b$ -side of the contour  $\mathcal{C}^{(1)}(a, b, c)$ , we get the region  $DR_{\bar{f}, \bar{e}, \bar{d}}^{(1)}$  (see the top row in Figure 4.1). Thus,

$$M(DR_{a,b,c}^{(1)}) = M(DR_{\bar{f}, \bar{e}, \bar{d}}^{(1)}).$$

On the other hand, by the definition of function  $\Phi$ , we obtain  $\Phi(a, b, c) = \Phi(\bar{f}, \bar{e}, \bar{d})$ . Therefore, to prove (4.1), it suffices to verify that

$$M(DR_{\bar{f}, \bar{e}, \bar{d}}^{(1)}) = \Phi(\bar{f}, \bar{e}, \bar{d}). \quad (4.3)$$

If  $\bar{e} \leq 4$ , then the triple  $(\bar{f}, \bar{e}, \bar{d})$  are among the ones in the base cases, and (4.3) holds. Thus, we can assume that  $\bar{e} \geq 5$ . We now want to show that  $(\bar{f}, \bar{e}, \bar{d}) \in \bar{\mathcal{D}}_1$ , then (4.3) follows from the Case 1 treated above. It is more convenient to re-write  $\mathcal{D}_1$  with all constraints in terms of  $a, b, c$  as

$$\begin{aligned} \bar{\mathcal{D}}_1 = \{ \mathcal{P}^{(1)}(a, b, c) = k, b \geq 5, 2b - a - 2c + 1 \geq 0, \\ 3b - 2a - 2c + 1 \geq 0, 2b - a - c + 1 \geq 3, 2 \leq a \leq 2b - a - c + 1 \}. \end{aligned} \quad (4.4)$$

The above flip does not change the perimeter, so the first constraint holds. Since we assuming  $\bar{e} \geq 5$ , the second constraint also holds here. Next, we have  $2\bar{e} - \bar{f} - 2\bar{d} + 1 = c \geq 0$ ,  $3\bar{e} - 2\bar{f} - 2\bar{d} + 1 = b \geq 0$ , and  $2\bar{e} + \bar{f} - \bar{d} + 1 = c + \bar{d} \geq 3$ . Moreover,  $\bar{f} = c + \bar{d} - a + 1 \geq c + \bar{d} \geq 3$ , and the condition  $\bar{f} \leq 2\bar{e} - \bar{f} - \bar{d} + 1$  is equivalent to  $a \geq 0$ , which is obviously true. This means that  $(\bar{f}, \bar{e}, \bar{d})$  is indeed in  $\bar{\mathcal{D}}_1$ .

Similarly, if  $(a, b, c) \in \tilde{\mathcal{D}}_2$ , we also flip  $DR_{a,b,c}^{(2)}$  over the  $b$ -side of the contour  $\mathcal{C}^{(2)}(a, b, c)$  and get  $DR_{\tilde{f}, \tilde{e}, \tilde{d}}^{(2)}$ . Then (4.2) follows again from Case 1.

*Case 3:*  $(a, b, c) \in \bar{\mathcal{D}}_3 \cup \tilde{\mathcal{D}}_3$ .

Assume that  $(a, b, c) \in \bar{\mathcal{D}}_3$ .

If  $c \geq 2$ , then  $M(DR_{a,b,c}^{(1)})$  and  $\Phi(a, b, c)$  satisfy the same recurrence (R1); and if  $c = 1$ , then the later functions both satisfy the recurrence (R2). Then (4.1) follows from the induction hypotheses. We also get (4.1) if  $(a, b, c) \in \bar{\mathcal{D}}_{3c}$  (in this case the first equality of (R3) has been used). Thus, (4.1) always holds when  $(a, b, c) \in \bar{\mathcal{D}}_3$ .

Arguing similarly, we have (4.2) holds when  $(a, b, c) \in \tilde{\mathcal{D}}_3$ .

*Case 4:*  $(a, b, c) \in \bar{\mathcal{D}}_4 \cup \tilde{\mathcal{D}}_4$ .

Similar to Case 2, we want to reduce this case to the cases treated before by flipping our region in a suitable way.

If  $(a, b, c) \in \bar{\mathcal{D}}_4$  (resp.  $\tilde{\mathcal{D}}_4$ ), we get  $DR_{b,a,\bar{f}}^{(1)}$  (resp.  $DR_{b,a,\bar{f}}^{(2)}$ ) by flipping the region  $DR_{a,b,c}^{(2)}$  (resp.  $DR_{a,b,c}^{(1)}$ ) about the horizontal line passing the western vertex (see the bottom row of Figure 4.1). It deduces that

$$M(DR_{a,b,c}^{(1)}) = M(DR_{b,a,\bar{f}}^{(2)}) \quad \text{and} \quad M(DR_{a,b,c}^{(2)}) = M(DR_{b,a,\bar{f}}^{(1)}).$$

On the other hand, by the definition of the functions  $\Phi$  and  $\Psi$ , we have

$$\Phi(a, b, c) = \Psi(b, a, \bar{f}) \quad \text{and} \quad \Psi(a, b, c) = \Phi(b, a, \bar{f}).$$

Therefore, we only need to verify that

$$M(DR_{b,a,\bar{f}}^{(1)}) = \Phi(b, a, \bar{f}) \quad \text{and} \quad M(DR_{b,a,\bar{f}}^{(2)}) = \Psi(b, a, \bar{f}). \quad (4.5)$$

Let us prove the first equality in (4.5). Similar to Case 2, by the base cases, we can assume  $a \geq 7$  and  $\bar{e} + \bar{f} \geq 3$ . However, now, we can check easily that  $(b, c, \bar{f}) \in \bar{\mathcal{D}}_3$  or  $\bar{\mathcal{D}}_1 \cup \bar{\mathcal{D}}_2$  if  $c = 1$  or  $0$ , respectively. Then the first equality in (4.5) follows from the cases treated before. Do similarly for the second equality in (4.5). This finishes our proof.

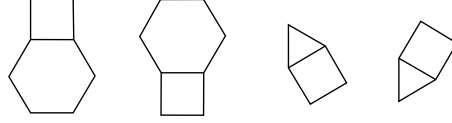


Figure 5.1: All types of tiles having weight 1 in the regions  $DR_{a,b,c}^{(i)}(x)$ 's.

## 5 More applications of the method.

In this section, we point out several further applications of the method using in the proof of Theorem 2.1.

Consider the weighted version  $DR_{a,b,c}^{(i)}(x)$  of the dragon region  $DR_{a,b,c}^{(i)}$  by assigning all tiles in Figure 5.1 a weight 1, and each of other tiles an indeterminate weight  $x > 0$ . Now,  $M(DR_{a,b,c}^{(i)}(x))$  is the sum of weights of all tilings in  $DR_{a,b,c}^{(i)}(x)$ , where the weight of a tiling is the product of weights of its constituent tiles.

**Theorem 5.1.** (a) Assume that  $a$ ,  $b$ , and  $c$  are three non-negative integers satisfying  $b \geq 2$ ,  $\bar{d} := 2b - a - 2c + 1 \geq 0$  and  $\bar{e} := 3b - 2a - 2c + 1 \geq 0$ . Then

$$M\left(DR_{a,b,c}^{(1)}(x)\right) = 2^{\frac{(a-b)(a-b-1)}{2}}(x^2 + 1)^A(x^2 + 2)^B x^C, \quad (5.1)$$

where

$$A = (b - c + 1)(2b - a - c) + \frac{(b-a)(b-a-1)}{2},$$

$$B = \frac{(a-b+c)(a-b+c-1)}{2},$$

$$\text{and } C = (a - b - 1)^2 + (a - b + c - 1)(a - b + c) - c + \min(2a - 2b + c - 1, 0).$$

(b) Moreover, if  $\tilde{d} := 2b - a - 2c - 1 \geq 0$  and  $\tilde{e} := 3b - 2a - 2c - 1 \geq 0$ , then

$$M\left(DR_{a,b,c}^{(2)}(x)\right) = 2^{\frac{(b-a)(b-a-1)}{2}}(x^2 + 1)^{A'}(x^2 + 2)^{B'} x^{C'}, \quad (5.2)$$

where

$$A' = (b - c - 1)(2b - a - c) + \frac{(a-b)(a-b-1)}{2},$$

$$B' = \frac{(a-b+c)(a-b+c+1)}{2},$$

$$\text{and } C' = (b - a - 1)^2 + (a - b + c + 1)(a - b + c) - \max(2a - 2b + c + 1, 0).$$

We omit the proof of Theorem 5.1 here, because it is essentially the same as the proof of Theorem 2.1.

Next, we conclude the paper by introducing two new families of regions, which has the number of tilings given also by powers of 2 and 3.

Searching over various families of regions having similar structure to the Aztec diamonds [3], we find several ones, in which the tilings are enumerated by a powers of 2 and 3. One of these families is the “needle rhombi” introduced by the author (see Theorem 25 [5]). Figure 5.2 shows the needle rhombus of order 3. Inspired by the dragon regions, we generalize the later regions to two new families of regions as follows.

Partition the triangular lattice into equilateral triangles of side 3, which we call *basic triangles*. Remove all six lattice segments opposite to each vertex of those basic triangles. We get a new lattice, which the needle rhombi live in. Similar to the contours  $\mathcal{C}^{(i)}(a, b, c)$ , we consider



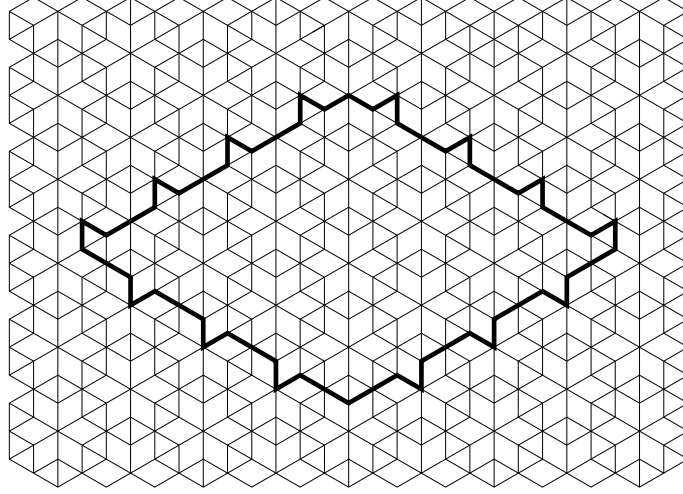


Figure 5.2: The needle rhombus  $R_3$ .

a six-sided contour  $\mathcal{C}(a, b, c)$  along the sides of the above basic triangles having side-lengths  $a, b, c, d := 2b - a - 2c, e := 3b - 2a - 2c, f := |2b - 2a - c|$  (the unit here is the side-length of the basic triangles). Define a two families of *needle regions*  $N_{a,b,c}^{(1)}$  and  $N_{a,b,c}^{(2)}$  restricted by the above contour as in Figures 5.3(a) and (b) for the case  $a > c + d$ , and Figures 5.3(c) and (d) for the case  $a \leq c + d$ .

By repeating the process in enumerating the tilings of the dragon regions, we get the following tiling formulas for the needle regions.

**Theorem 5.2.** *Assume that  $a, b$ , and  $c$  are three non-negative integers satisfying  $b \geq 2$ ,  $2b - a - 2c \geq 0$  and  $3b - 2a - 2c \geq 0$ . Then*

$$\begin{aligned} M(N_{a,b,c}^{(1)}) &= 2^{a^2-3ab+3b^2-3bc+c^2+ac+a-b+\frac{c}{2}-\frac{1}{2}|2a-2b+c|} \\ &\quad \times 3^{(5a-7b+5c+1)(a-b+c)/2+b(b-1)-ac} \end{aligned} \quad (5.3)$$

and

$$\begin{aligned} M(N_{a,b,c}^{(2)}) &= 2^{a^2-3ab+3b^2-3bc+c^2+ac+a-b+\frac{c}{2}-\frac{1}{2}|2a-2b+c|} \\ &\quad \times 3^{(5a-7b+5c+1)(a-b+c)/2+b(b-1)-ac+(b-a)+\min(2a-2b+c,0)}. \end{aligned} \quad (5.4)$$

The proof of Theorem 5.2 will be left to reader.

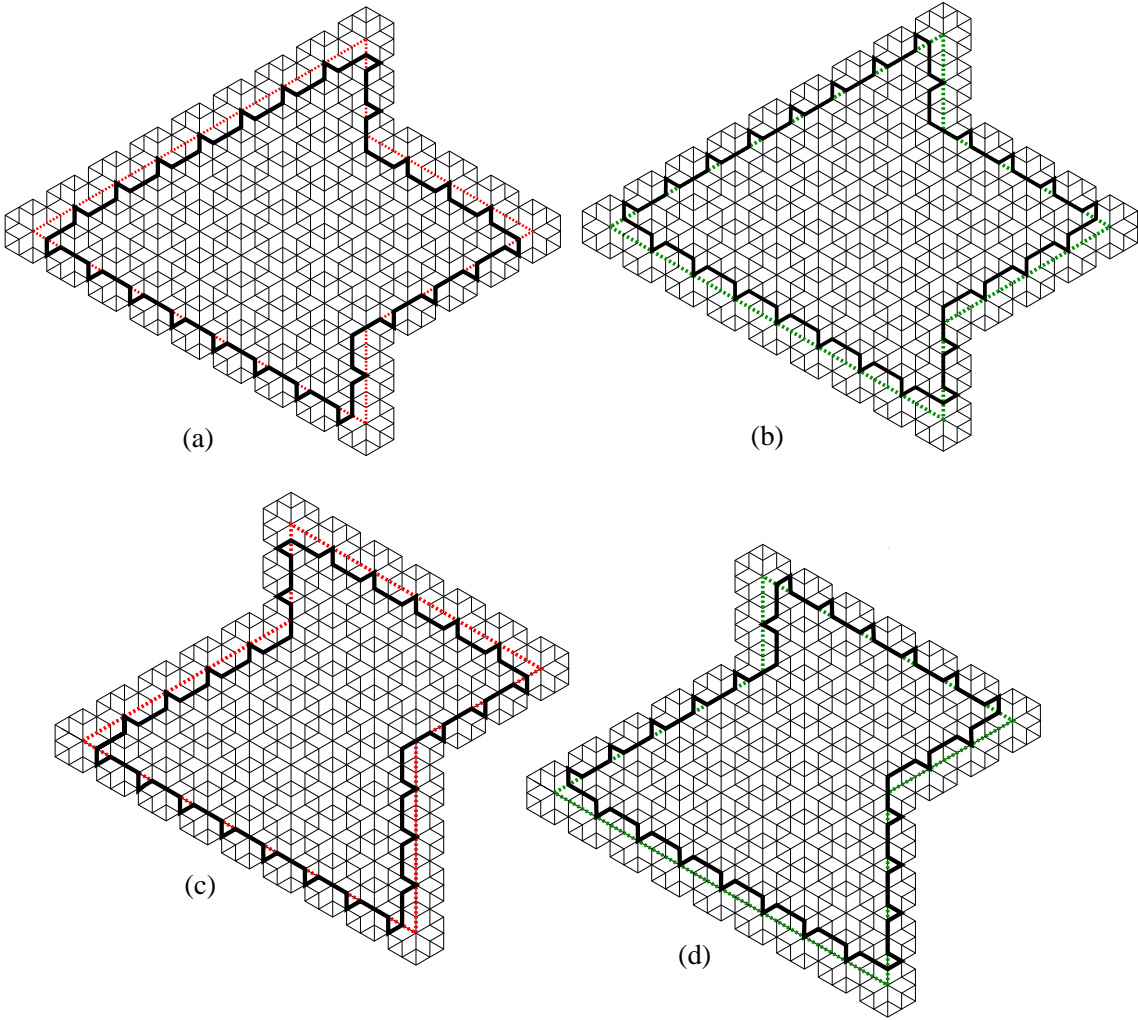


Figure 5.3: The regions (a)  $N_{8,8,2}^{(1)}$ , (b)  $N_{8,8,2}^{(2)}$ , (c)  $N_{5,8,4}^{(1)}$  and (d)  $N_{5,8,4}^{(2)}$ .

## References

- [1] M. Ciucu, *Perfect matchings and perfect powers*, J. Algebraic Combin. **17** (2003), 335–375.
- [2] C. Cottrell and B. Young, *Domino shuffling for the Del Pezzo 3 lattice*, arXiv:1011.0045. <http://arxiv.org/abs/1011.0045>
- [3] N. Elkies, G. Kuperberg, M.Larsen, and J. Propp, *Alternating-sign matrices and domino tilings*, J. Algebraic Combin. **1** (1992), 111–132, 219–234.
- [4] E. H. Kuo, *Applications of Graphical Condensation for Enumerating Matchings and Tilings*, Theor. Comput. Sci. **319** (2004), 29–57.
- [5] T. Lai, *New aspects of regions whose tilings are enumerated by perfect powers*, Elec. J. of Combin. **20** (4) (2013), P31.
- [6] M. Leoni, G. Misiker, S. Neel, and P. Turner *Aztec Castles and the  $dP_3$  Quiver*, arXiv:1308.3926. [texttthttp://arxiv.org/abs/1308.3926](http://arxiv.org/abs/1308.3926)
- [7] J. Propp, *Enumeration of matchings: Problems and progress*, New Perspectives in Geometric Combinatorics, Cambridge Univ. Press, 1999, 255–291.
- [8] S. Zhang, *Cluster algebra and perfect matchings of subgraphs of the  $dP_3$  lattice*, 2012. URL: <http://www.math.umn.edu/reiner/REU/Zhang2012.pdf>